Robotica (2015) volume 33, pp. 225–239. © Cambridge University Press 2014
doi:10.1017/S0263574714000307

A Lyapunov controller for self-balancing two-wheeled vehicles

A. Maddahi, A. H. Shamekhi* and A. Ghaffari

Department of Mechanical Engineering, K. N. Toosi University of Technology, Tehran, Iran

(Accepted February 2, 2014. First published online: March 5, 2014)

SUMMARY

Segway is a self-balancing motorized two-wheeled vehicle which is able to carry the human body. The main issue in design of such a vehicle is to choose a stable control system capable of keeping the rider close to the upright position over smooth and non-smooth surfaces. This work extends the research previously performed by the authors for design of a controller, using the feedback linearization technique, to increase the stability of a two-wheeled vehicle carrying human. This paper investigates the design and validation of a controller for an inertial mobile vehicle using the Lyapunov's feedback control design technique. The system equations of motion are derived followed by finding the Lyapunov function required to design the controller. Owing to the discontinuity, originating from a sign function in the control law, the proposed control system is discontinuous. Therefore, the existence, continuity, and uniqueness of the solution are proven utilizing the Filippov's solution. Afterwards, the asymptotic stability of the control system is proven using the extensions of Lyapunov's stability theory to nonsmooth systems, and LaSalle's invariant set theorem. Finally, the effectiveness of the proposed control system is validated using simulation studies. Results confirm that the controller keeps the system stable while provides good position tracking responses.

KEYWORDS: Segway; Two-wheeled vehicle; Filippov's solution; Lyapunov controller.

Nomenclature

θ	Tilt angle of link with respect to Z_R-axis [rad]
J_b	Moment of inertia of combination of link, seat, human, and base with respect to Z_R-axis [kg.m^2]
J_w	Moment of inertia of each wheel about Z_R-axis [kg.m^2]
I_w	Moment of inertia of each wheel about Y_R-axis [kg.m^2]
m_w	Mass of each wheel [kg]
m_l	Combined mass of human body, link and seat [kg]
I_l	Link moment of inertia with respect to Y_R-axis passing from its center of mass [kg.m^2]
$\dot{x}$	Linear velocity of base along X_R direction [m/s]
$\dot{y}$	Linear velocity of base along Y_R direction [m/s]
$\dot{z}$	Linear velocity of vehicle along Z_R direction [m/s]
M	Mass of entire vehicle [kg]
β	Angular displacement of link with respect to upright position [rad]
R	Radius of each wheel [m]
$2d$	Wheelbase [m]
$\ddot{\varphi}_L$,$\ddot{\varphi}_R$	Angular accelerations of left and right wheels [rad/s^2]
a	Distance between center of mass and joint of link [m]

* Corresponding author. E-mail: shamekhi@kntu.ac.ir

https://doi.org/10.1017/S0263574714000307 Published online by Cambridge University Press

1. Introduction

Two-wheeled mobile vehicle is a machine whose movement is based on two separately driven wheels placed on either side of the robot body. Using two-wheeled mechanism, the vehicle is capable of changing its direction by varying the relative angular velocity of wheels; and hence, does not require an additional steering motion. During the vehicle motion, the center of rotation may fall anywhere in the line joining the wheels together (wheelbase).[1,2] This uncertainty causes inaccuracies, and is more challenging when the vehicle carries an inertial and massy body such as human. A solution, to increase the accuracy, is to design a stabilizing controller which is capable of keeping the robot along desired situations.

Recently, the self-balancing two-wheeled vehicles have been undergoing a considerable development. Extensive research activities have subsequently been performed on the design and control of these vehicles. The primary commercial generation of two-wheeled vehicles was manufactured by Segway Inc. in 2002.[3] This vehicle is known as "Segway". The idea of controlling the Segway has been inspired from the control of inverted pendulum.[4–6] Yuta *et al.*[7,8] controlled a vehicle subsystem for an autonomous mobile robot with power wheeled steering. Grasser *et al.*[9] developed a small two-wheeled robot system, which was hard to control due to small values of normal friction force and light weight of attached pendulum. Lee and Jung[10] proposed a sensor fusion technique to measure the balancing angle of the inverted pendulum robot system using Kalman filter.

With respect to the application, there exist considerable efforts on two-wheeled vehicles featuring the ability of transporting the human. For this purpose, the comfort and safety of the rider on the vehicle are the main concerns which result in having reliable control laws for the system. Since these vehicles have two wheels and the rider must be kept in upright position, the stability problem is one of the important challenges. As far as the accurate control of two-wheeled vehicles is concerned, Azizan *et al.*[11] developed a hierarchical intelligent control scheme for a two-wheeled human transportation vehicle. Tsai *et al.*[12] presented an adaptive neural network control for a self-balancing scooter. They utilized a radial basis function neural network model to control the scooter. Vermeiren *et al.*[13] prototyped a model of Segway called "B2," which was able to carry the human in the street. The advantage of "B2" was the ability to negotiate through narrow city streets. Aracil *et al.*[14] developed a Takagi-Sugeno fuzzy model from the effective prototype parameters. However, the linear control laws, exerted on Segway, had good practical features and the analytically-estimated domain of attraction was extremely small. Maddahi and Shamekhi[15] developed a scheme to control two-wheeled vehicles carrying a massy and inertial body. This system comprised a differentially-driven mechanism with two wheels and a main body connecting the wheels to each other. The control law, required to drive motors, was designed using the feedback linearization technique. In addition to having stability on smooth surfaces, the system was shown to behave stably on nonsmooth surfaces.[15]

To the best of authors' knowledge, researches on adopting the Lyapunov technique to find a stable controller for two-wheeled self-balancing vehicles, carrying a human, are sparse. This paper, for the first time, addresses the design process of a stable Lyapunov controller for such a vehicle capable of transporting a human. The system equations of motion are first derived, followed by derivation of control law using Lyapunov feedback control design technique. Since, the control law includes discontinuity terms, the existence, continuation, and uniqueness of Filippov's solution to the system are proven. Finally, consequences of simulation studies are carried out in order to verify the proposed control law. As compared to work done by the authors,[15] the current study uses the Lyapunov technique and Filippov's solution to find the controller.

The organization of this paper is as follows. Section 2 describes the dynamic equations of two-wheeled vehicle. Section 3 presents design of the controller. The stability analysis of the design controller is investigated in Section 4. Section 5 reports simulation results including test of the system along various smooth and non-smooth trajectories. Section 6 outlines conclusions and future work.

2. Dynamic Modeling

The overall view of a two-wheeled self-balanced vehicle is shown in Fig. 1. As observed, the posture of human with respect to the vehicle is modeled by a seat and a 1-DOF link attached to the vehicle center of mass. The link is controlled by applying torque T to the link actuator, and is not fixed to the wheelbase. In this model, only rolling resistance is supposed between wheels and the movement

https://doi.org/10.1017/S0263574714000307 Published online by Cambridge University Press

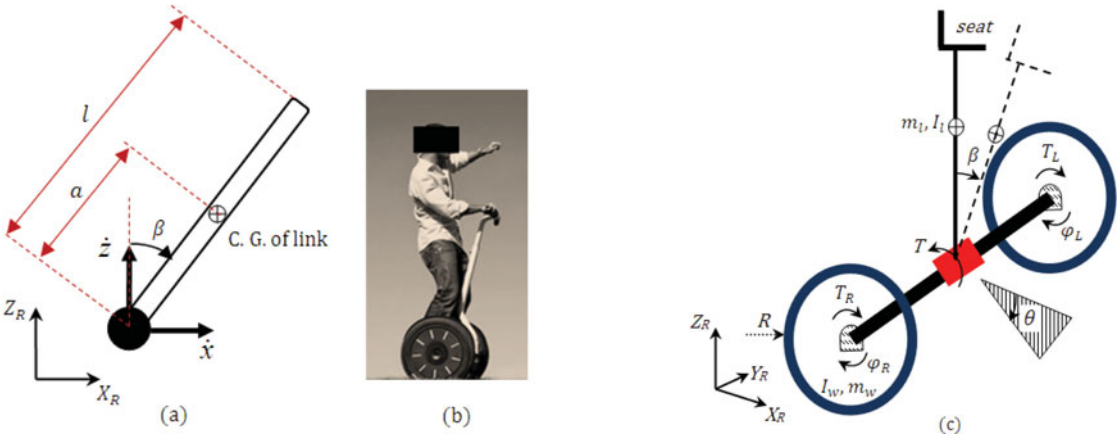


Fig. 1. (Colour online) Coordinate systems of two-wheeled self-balancing vehicle: (a) 2D view of modeled Segway; (b) Real model of Segway and the rider; (c) 3D view of system.

surface. The total kinetic energy of the system, K, is expressed by:

$$K = \frac{1}{2}\left[I_w\left(\dot{\varphi}_L^2 + \dot{\varphi}_R^2\right) + \left(J_b + 2J_w + 2m_w d^2\right)\dot{\theta}^2 + (m_b + 2m_w)(\dot{x}^2 + \dot{y}^2) + M\dot{z}^2 + m_l V_l^2 + I_l(\dot{\beta})^2\right] \tag{1}$$

where $m_b = M - 2m_w$. Note that V_l symbolizes the linear velocity of the link center of mass and is given by:

$$V_l^2 = (\dot{x}\cos\theta + \dot{y}\sin\theta + a\dot{\beta}\cos\beta)^2 + (-\dot{x}\sin\theta + \dot{y}\cos\theta)^2 + (\dot{z} - a\dot{\beta}\sin\beta)^2 \tag{2}$$

As presented in (2), the direction of V_l depends on two velocities: the base velocity ($\dot{x}\cos\theta + \dot{y}\sin\theta$,$-\dot{x}\sin\theta + \dot{y}\cos\theta$ and $\dot{z}$), and the velocity originating from the angular displacement of link with respect to upright position ($a\dot{\beta}\cos\beta$ and $-a\dot{\beta}\sin\beta$).

The potential energy, U, of the system is calculated using:

$$U = m_l g a[1 - \cos(\beta)] \tag{3}$$

where g is the gravitational acceleration.

By using Lagrangian method, the system's equations of motion, in two-dimensional movement, are obtained using (1) to (3) as follows:

$$(m_b + 2m_w)\ddot{x}\cos\theta + (m_b + 2m_w)\ddot{y}\sin\theta + \frac{I_w}{R}(\ddot{\varphi}_L + \ddot{\varphi}_R) = \frac{1}{R}(T_L + T_R) \tag{4a}$$

$$(J_b + 2J_w + 2m_w d^2)\ddot{\theta} + \frac{I_w.d}{R}(\ddot{\varphi}_R - \ddot{\varphi}_L) = \frac{d}{R}(T_R - T_L) \tag{4b}$$

$$\left(m_l a^2 + I_l\right)(\ddot{\beta}) + m_l a(\ddot{x}\cos\theta + \ddot{y}\sin\theta)\cos\beta + m_l a\dot{\theta}(\dot{y}\cos\theta - \dot{x}\sin\theta)\cos\beta - ma\,(\ddot{z} - g)\sin(\beta) = T \tag{4c}$$

where T is the control torque required to move the link along the desired trajectory. T_L and T_R denote the torques imposed on the left and right wheels, respectively. $\ddot{z}$ is the vertical acceleration that the surface applies to the vehicle. It is obvious that $\ddot{z} = 0$ when the surface is smooth and parallel with the horizontal surface.

https://doi.org/10.1017/S0263574714000307 Published online by Cambridge University Press

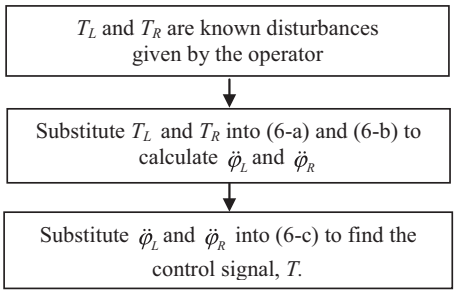


Fig. 2. Flowchart defined to design stable controller, T. Control signal keeps link along upright position, that is, to reach equilibrium point at $\beta = 0$.

Also, the constraint equations are obtained as Eqs. (5a)–(5c).

$$\ddot{x}\cos\theta + \ddot{y}\sin\theta = R\ddot{\varphi}_L + d\ddot{\theta} \tag{5a}$$

$$\ddot{x}\cos\theta + \ddot{y}\sin\theta = R\ddot{\varphi}_R - d\ddot{\theta} \tag{5b}$$

$$\dot{y}\cos\theta - \dot{x}\sin\theta = 0 \tag{5c}$$

Combining Eqs. (4a) to (5c) results in the following dynamic equations:

$$\left[(m_b + 2m_w)\frac{R}{2} + \frac{I_w}{R}\right](\ddot{\varphi}_L + \ddot{\varphi}_R) = \frac{1}{R}(T_L + T_R) \tag{6a}$$

$$[(J_b + 2J_w + 2m_w d^2)\frac{R}{2d} + \frac{I_w.d}{R}](\ddot{\varphi}_R - \ddot{\varphi}_L) = \frac{d}{R}(T_R - T_L) \tag{6b}$$

$$\left(m_l a^2 + I_l\right)(\ddot{\beta}) + \left(m_l a\frac{R}{2}\right)(\ddot{\varphi}_L + \ddot{\varphi}_R)\cos\beta - ma\,(\ddot{z} - g)\sin(\beta) = T \tag{6c}$$

As shown in Fig. 1(c), an actuator is considered to control position of the link operating independently of the wheel actuators. Since the controller is designed to keep the link along upright position, Eq. (6c) is of concern in finding the controller torque T. In other words, torques T_L and T_R, which are determined by the rider, are assumed as known disturbances in Eqs. (6a) and (6b). Next, two time-dependent disturbances ($\ddot{\varphi}_L$ and $\ddot{\varphi}_R$) are obtained and utilized in Eq. (6c). Figure 2 flowcharts the procedure defined to design the controller.

The state space model for Eq. (6c) is derived by setting the following states:

$$\begin{cases} x_1 = \beta \\ x_2 = \dot{\beta} \end{cases} \tag{7}$$

The state space model is defined as follows:

$$\begin{aligned} \dot{x}_1 &= x_2 = f_1 \\ \dot{x}_2 &= \frac{1}{A}[T - B(\ddot{\varphi}_L + \ddot{\varphi}_R) + m_l a(\ddot{z} - g)\sin(x_1)] = f_2 \end{aligned} \tag{8}$$

https://doi.org/10.1017/S0263574714000307 Published online by Cambridge University Press

Note that the right hand sides of the state space equations are called f_1 and f_2 for further simplifications. In (8), the parameters A and B are given by:

$$A = I_l + m_l a^2$$
$$B = \left(m_l \frac{R}{2} a\right) \cos(x_1) \tag{9}$$

3. Lyapunov Feedback Control System

The Lyapunov feedback control design technique is employed to find the control signal (torque) of link, T. The state space model, presented in Eq. (8), is now employed to design a stabilizing feedback. Indeed, we aim at designing a Lyapunov controller to perform regulatory task which is defined as giving specific equilibrium angle determining the desired angle between the link axis and the upright position while the two-wheeled vehicle is moving. The main goal of the control system is to asymptotically approach the equilibrium point, and then remain stable there. The control law is derived using a nonstraightforward process recommended in ref. [16]. This process is directly influenced by chosen Lyapunov function. Note that the Lyapunov function of the system (V) and its derivative ($\dot{V}$) are firstly derived while the derivative function includes the control law T. Therefore, the control law should be manipulated to make the derivative of Lyapunov function semi-negative. Equation (10) presents the control law proposed for the Lyapunov function.

$$\begin{aligned} T = & -k_1 x_1 x_2 \left|\ddot{z} - g\right| \operatorname{sgn}(x_1) - k_2 x_2 + m_l a x_2 \left|\ddot{z} - g\right| \sin(x_1) - x_1 \\ & + B(\ddot{\varphi}_L + \ddot{\varphi}_R) - m_l a(\ddot{z} - g) \sin(x_1) \end{aligned} \tag{10}$$

where k_1 and k_2 are the proportional and derivative gains of the controller. The proposed controller is discontinuous due to term $sgn(x_1)$. The function $sgn(x_1)$ is the sign function and defined as follows:

$$\operatorname{sgn}(x_1) = \begin{cases} +1 & x_1 > 0 \\ 0 & x_1 = 0 \\ -1 & x_1 < 0 \end{cases} \tag{11}$$

By replacing T into (8), the following state space equations are resulted:

$$\begin{aligned} \dot{x}_1 &= x_2 = f_1 \\ \dot{x}_2 &= \frac{1}{A}[-k_1 x_1 x_2 \left|\ddot{z} - g\right| \operatorname{sgn}(x_1) - k_2 x_2 + m_l a x_2 \left|\ddot{z} - g\right| \sin(x_1) - x_1] = f_2 \end{aligned} \tag{12}$$

The nonsmooth systems violate the basic assumption of solution theories of ordinary differential equations which results in not fulfilling the Lipschitz-continuous requirements. For this system, before proposing any solution, the existence, uniqueness, and stability must be discussed. One of the most straightforward methods used to analyze the nonsmooth systems is Filippov's solution.[17,18] Using Filippov's solution concept and Clarke's generalized gradient, the Lyapunov stability theory is developed for smooth systems and then extended to nonsmooth systems.[16,19,20] Finally, the stability of the system is investigated.

4. Stability Analysis

The Filippov's solution is used to prove the existence, uniqueness, and continuity of nonsmooth systems.[17] Next, a smooth Lyapunov function for the nonsmooth system is constructed, and the global asymptotic stability of the system is proven.[16]

As seen, Eq. (12) includes a nonlinear differential equation with a discontinuous term which originates from the term $sgn(x_1)$ in the proposed control law. Using the Filippov's solution, the

https://doi.org/10.1017/S0263574714000307 Published online by Cambridge University Press

discontinuity surface of the system, described in Eq. (12), is:

$$S := \{\vec{x} : x_1 = 0\} \tag{13}$$

The discontinuity surface, S, divides the solution region into two regions, Ω^+ and Ω^-.

$$\Omega^+ := \{\vec{x} : x_1 > 0\}, \Omega^- := \{\vec{x} : x_1 < 0\} \tag{14}$$

The right-hand sides of (12), which are measurable and bounded, are piecewise continuous and defined everywhere in Ω. Thus, the condition B of Filippov's solution is satisfied. Moreover, the local existence and continuity of solutions exist according to theorems 4 and 5 of Filippov.[17] Consider the discontinuity surface (S) is smooth and independent of time. Since, the right-hand side of Eq. (12) is continuous in small regions before and after S, it satisfies the conditions A, B and C of Filippov's solution (See Appendix).[17] Let assume the limiting values of the vector function of Eq. (12), when S approaches from Ω^+ and Ω^-, are defined by f_s^+ and f_s^-.[17] Therefore, the following formulations can be written for the system:

$$f_s^+ \begin{cases} \dot{x}_1 = x_2 \\ \dot{x}_2 = \frac{1}{A}[-k_1 x_1 x_2 \,|\ddot{z} - g| - k_2 x_2 + m_l a x_2 \,|\ddot{z} - g| \sin(x_1) - x_1] \end{cases} \tag{15}$$

and,

$$f_s^- \begin{cases} \dot{x}_1 = x_2 \\ \dot{x}_{22} = \frac{1}{A}[+k_1 x_1 x_2 \,|\ddot{z} - g| - k_2 x_2 + m_l a x_2 \,|\ddot{z} - g| \sin(x_1) - x_1] \end{cases} \tag{16}$$

Projections of f_s^+ and f_s^- along the normal to the discontinuity surface, f_{Ns}^+ and f_{Ns}^- are given by:[17]

$$\begin{aligned} f_{Ns}^+ &= f_s^+ \cdot N_s \\ f_{N_s}^- &= f_s^- \cdot N_s \end{aligned} \tag{17}$$

where $N_S = \begin{Bmatrix} 1 & 0 \end{Bmatrix}^T$.

In conclusion,

$$\begin{aligned} f_{N_s}^+ &= x_2 \\ f_{N_s}^- &= x_2 \end{aligned} \tag{18}$$

In (18), both f_{Ns}^+ and f_{Ns}^- have the same sign, which means that the conditions of Lemma 9 of Filippov's solution are automatically satisfied (see Appendix). Thus, we have uniqueness and continuous dependence of the solution on the initial conditions in the domain $\Omega^- + S + \Omega^+$.

For the stability analysis, the extension of Lyapunov's second method to nonsmooth dynamic systems is employed.[16] A smooth Lyapunov function for the existing nonsmooth dynamic system is considered. The system has the following equilibrium point. Note that the system can be either autonomous or nonautonomous.

$$\vec{x}_{eq} = [\, x_{1eq} \quad x_{2eq} \,]^T = [\, 0 \quad 0 \,]^T \tag{19}$$

Equation (12) can be rewritten in the following form:[21]

$$\begin{cases} L_1 = \dot{x}_1 - f_1 = 0 \\ L_2 = \dot{x}_2 - f_2 = 0 \end{cases} \tag{20}$$

https://doi.org/10.1017/S0263574714000307 Published online by Cambridge University Press

Let us define the following integral:[21]

$$I_i' = \int_0^t s_i L_i dt \quad (i = 1, 2) \tag{21}$$

Having the following continuous weighting functions of time:

$$\begin{aligned} s_1 &= x_1 \\ s_2 &= (I_l + m_l a^2) x_2 \end{aligned} \tag{22}$$

Equation (21) can be expressed, for $i = 1,2$ as follows:

$$I' = I_1' + I_2' = 0 \tag{23}$$

where,

$$I_1' = \int_0^t s_1 L_1 dt = \int_0^t x_1(\dot{x}_1 - f_1) dt \tag{24}$$

$$I_2' = \int_0^t s_2 L_2 dt = \int_0^t (I_l + m_l a^2) x_2(\dot{x}_2 - f_2) dt \tag{25}$$

Therefore,

$$I_1' = \frac{1}{2} x_1^2 - \int_0^t x_1 x_2 dt \tag{26}$$

and

$$\begin{aligned} I_2' &= \frac{(I_l + m_l a^2)}{2} . x_2^2 - \int_0^t (I_l + m_l a^2) x_2 f_2 dt \\ &= \frac{(I_l + m_l a^2)}{2} x_2^2 - \int_0^t x_2 T dt + \int_0^t B x_2(\ddot{\varphi}_L + \ddot{\varphi}_R) dt - \int_0^t m_l a(\ddot{z} - g) x_2 \sin(x_1) dt \end{aligned} \tag{27}$$

The term I' can alternatively be rearranged as follows:[21]

$$I' = \sum\nolimits_{i=1}^{2} I_i' = F(t, x_1, x_2) + \int_0^t G(t, x_1, x_2) dt = 0 \tag{28}$$

To derive the Lyapunov function and corresponding derivative, based on the method proposed in ref. [21], the following equation is compared with Eq. (28).

$$V(t, x_1, x_2) + \int_0^t -\dot{V}(t, x_1, x_2) dt = 0 \tag{29}$$

Thus,

$$\begin{aligned} V(t, x_1, x_2) &= F(t, x_1, x_2) \\ \dot{V}(t, x_1, x_2) &= -G(t, x_1, x_2) \end{aligned} \tag{30}$$

https://doi.org/10.1017/S0263574714000307 Published online by Cambridge University Press

Equations (23) to (30) lease the Lyapunov function with the following form:

$$V = \frac{1}{2}x_1^2 + \frac{(I_l + m_l a^2)}{2}x_2^2 > 0 \tag{31}$$

As shown, the Lyapunov function is positive definite. The derivative of Lyapunov function with respect to time is expressed as:

$$\dot{V} = -x_2\left[-T - x_1 + B(\ddot{\varphi}_L + \ddot{\varphi}_R) - m_l a(\ddot{z} - g)\sin(x_1)\right] \tag{32}$$

By replacing the control law from (10) into (32), $\dot{V}$ is obtained negative semi-definite provided that $k_1 > m_l a$. To prove the negativity of the derivative of Lyapunov function, Eqs. (10) and (32) are combined. Therefore,

$$\dot{V} = -k_1 x_1 x_2^2\,|\ddot{z} - g|\,\mathrm{sgn}(x_1) - k_2 x_2^2 + m_l a x_2^2\,|\ddot{z} - g|\sin(x_1) \tag{33}$$

Since $x_1\mathrm{sgn}(x_1) = |x_1|$; thus,

$$\dot{V} = -k_1 x_2^2\,|\ddot{z} - g|\,|x_1| - k_2 x_2^2 + m_l a x_2^2\,|\ddot{z} - g|\sin(x_1) \tag{34}$$

and

$$\dot{V} = -k_2 x_2^2 - x_2^2\,|\ddot{z} - g|\,[k_1\,|x_1| - m_l a\sin(x_1)] \tag{35}$$

Considering $|x_1| > \sin(x_1)$ and by choosing $k_1 > m_l a$, we will have $k_1\,|x_1| > m_l a\sin(x_1)$. Finally, $\dot{V}$ becomes negative semi-definite. The control system is stable in the sense of Lyapunov, if the control gain k_1 is set greater than $m_l a$. Now, the asymptotic stability of the system is proven by employing nonsmooth version of invariant set theorems,[20,22] which is a common method to demonstrate the asymptotic stability when Lyapunov derivative is negative semi-definite over time.

Let L include the points located in the solution region Ω, where $\dot{V} = 0$; thus,

$$L = (\{x_1, x_2\}, \dot{V} = 0) \tag{36}$$

To show the asymptotic stability of the system, based on LaSalle's invariant sets theorem,[23] it is proven that the largest invariant set N, in set L, contains only the equilibrium point, $\vec{x}_{eq} = (0, 0)^T$. According to (32), $\dot{V} = 0$ requires, for all points in L, the following condition to be satisfied:

$$x_1 = x_2 = 0 \tag{37}$$

Let N contain a point where the error state x_2 is not zero. As shown in (38), at point $(0, x_2)$, by applying $x_1 = 0$ from (12), and assuming $x_2 \neq 0$, it is concluded that $\dot{x}_2 \neq 0$ which means the solution trajectory moves out of the set L and consequently set N. This contradicts the initial assumption that N is the largest invariant set in L. Thus, all points in set N should also satisfy $x_2 = 0$.

$$\dot{x}_2 = \frac{1}{A}(-k_2 x_2) \tag{38}$$

Using the same procedure, it is assumed that N includes a point where $x_1 \neq 0$. Thus, the largest invariant set N in L should only contain the equilibrium point shown by Eq. (19). Therefore, all solutions in Ω will converge to the equilibrium point. In conclusion, combination of the two-wheeled self-balancing vehicle and mounted link is asymptotically stable when the control law proposed in Eq. (10) is applied.

5. Simulation Study

Simulation study is carried out in order to demonstrate the asymptotic stability of the two-wheeled self-balanced model on which the proposed control law is exerted. Both Eqs. (10) and (12) are

https://doi.org/10.1017/S0263574714000307 Published online by Cambridge University Press

Table I. System parameters used in simulation study.

Parameter	Value
Moment of inertia of link with respect to C.G., I_l	3.1 kg.m^2
Mass of link, m_l	100 kg
Distance between the link C.G. and joint, a	0.6 m
Radius of the each wheel, R	0.15 m
Gravitational acceleration, g	9.81m/s^2
Angular acceleration of left and right wheels, $\ddot{\varphi}_L$,$\ddot{\varphi}_R$	Sin(t)

employed for numerical simulations, and 4th order Rounge-Kutta method is used as the integration routine. Table I lists the characteristics of the simulated vehicle and human. To show the applicability of the control law, the simulation studies are conducted while the vehicle moves on four different surfaces. In all cases, $\ddot{z}$ demonstrates the effect of the surface on the vehicle dynamic. The following initial conditions are chosen in all simulation scenarios:

$$\vec{x}_{\text{init}} = [\, x_{1\text{init}} \quad x_{2\text{init}} \,]^T = [\, 0.1 \quad 0 \,]^T \tag{39}$$

The controller gains are set to $k_1 = 80$, $k_2 = 2$. The value of control gain k_1 is always tuned to be greater than $m_l a$. In the first test, the vehicle is programmed to move on a horizontal and smooth surface. This simulation is to show how accurately the system can reach the equilibrium point when an arbitrary initial condition is given. Here, the parameters $\ddot{\varphi}_L$ and $\ddot{\varphi}_R$ are set to *sin* (t). As mentioned in Fig. (2), $\ddot{\varphi}_L$ and $\ddot{\varphi}_R$ are the effective parameters of the vehicle on the posture of the link. The reason of choosing $\ddot{\varphi}_L = \ddot{\varphi}_R = \sin(t)$is to consider a severe condition for the dynamic of vehicle while the effectiveness of the designed controller is examined.

5.1. Scenario I - smooth surface

Simulation results on the smooth surface are shown in Fig. 3. In this scenario, the smoothness of the surface is shown by $\ddot{z} = 0$ (see Fig. 3(a)). As observed, both angular displacement and angular velocity of the link reach the equilibrium point, that is, 0 rad and 0 rad/s (see Figs. 3(b) and (c)). This test validates the theoretical stability analysis performed earlier. As seen in Fig. 3(d), the control signal appeared smooth and continuous because of holding the continuity condition of the Filippov's solution.

Figures 3(e) and (f) illustrate the system Lyapunov function, V, and corresponding time-derivative function, $\dot{V}$. As shown, the Lyapunov function is always positive definite while $\dot{V}$ possesses the negative values. The values for both V and $\dot{V}$, when time is greater than 40 s, are very small (but not zero). However, they are still positive for V and negative for $\dot{V}$.

5.2. Scenario II- pulse surface

In the second scenario, the simulation is repeated when the vehicle is influenced by a pulse of vertical acceleration ($\ddot{z}$) applied by the surface (see Fig. 4(a)). Simulation results are shown in Fig. 4. As seen, the control law keeps the link close to the equilibrium point. The required control torque to keep the rider in upright position is depicted in Fig. 4(d). Furthermore, Figs. 4(e) and (f) verify the stability of the system while moving on pulse surface by appropriating negative values for $\dot{V}$.

5.3. Scenario III- incremental vertical acceleration

In the third set of validations, an incremental acceleration is imposed on the vehicle (see Fig. 5(a)). The angular displacement and velocity of the link approach zero values as shown in Figs. 5(b) and (c) which is desired. Figure 5(d) shows the opposite control signal to maintain the stability of the system while the vehicle moves on the surface that applies an increasing acceleration to vehicle tires. The negativity of the time-derivative of the Lyapunov function is depicted in Fig. 5(f).

https://doi.org/10.1017/S0263574714000307 Published online by Cambridge University Press

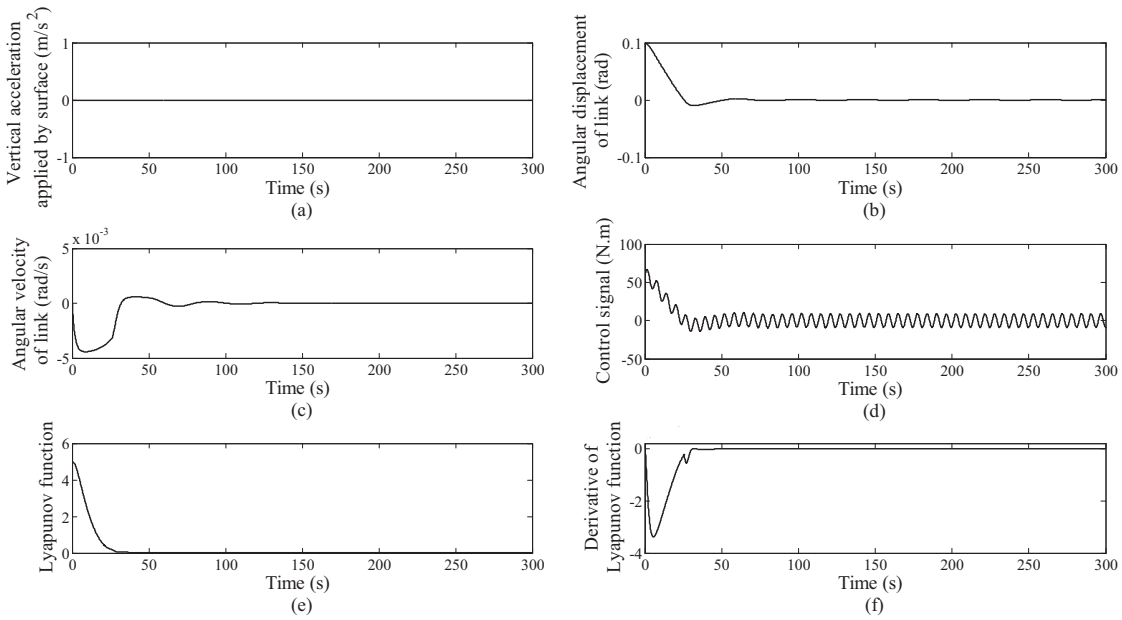


Fig. 3. Results of simulation study while vehicle moves on smooth surface; scenario I.

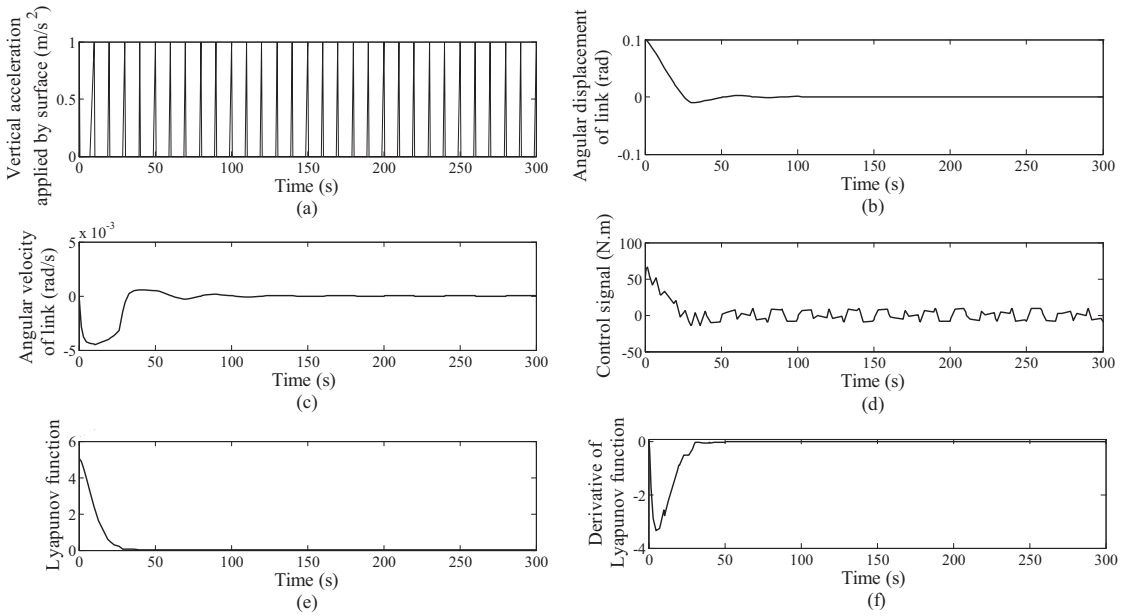


Fig. 4. Simulation results when the vehicle travels on pulse surface; scenario II.

5.4. Scenario IV- surface with random irregularities

Owing to the fact that an acceptable control law must guarantee the stability of the system in any situation, the next test is carried out by hypothesizing that the vehicle travels on a surface with irregularities. In this study, the vertical acceleration, exerted by the surface on the vehicle, imitates a random function such as one depicted in Fig. 6(a). With respect to Fig. 6(a), $\ddot{z}$ is randomly applied to the vehicle during motion. Looking at Figs. 6(b) and (c), the control signal (Fig. 6(d)) is shown to cause the link remains at its equilibrium point. Figures 6(e) and 5(f) indicate the Lyapunov function and its time-derivative are positive and negative during simulation, respectively. This confirms that

https://doi.org/10.1017/S0263574714000307 Published online by Cambridge University Press

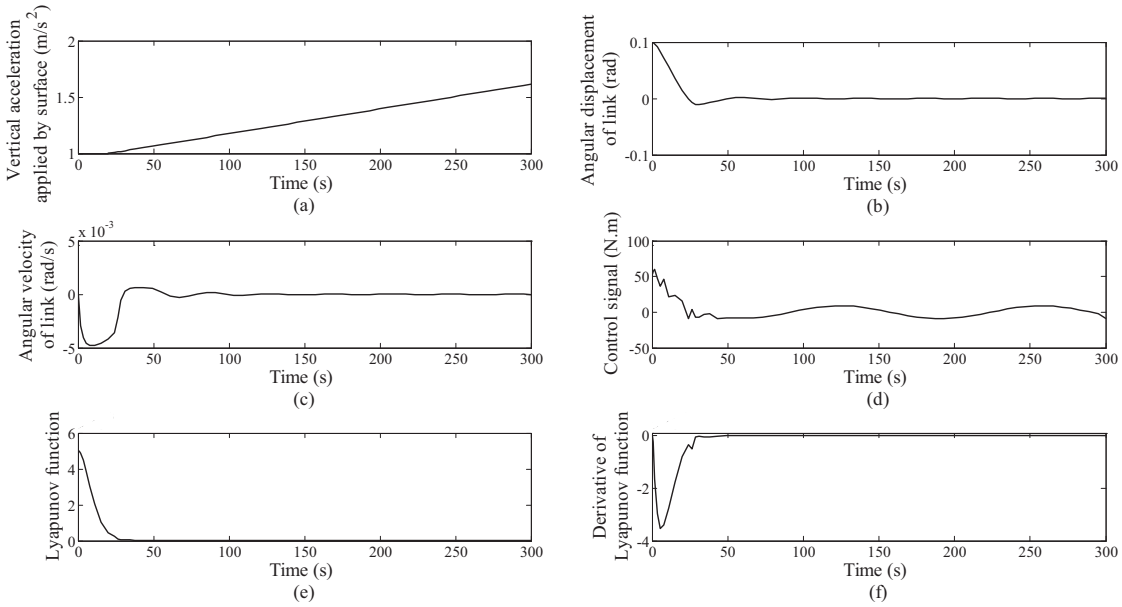


Fig. 5. Results of simulation study when incremental vertical acceleration is applied to vehicle; scenario III.

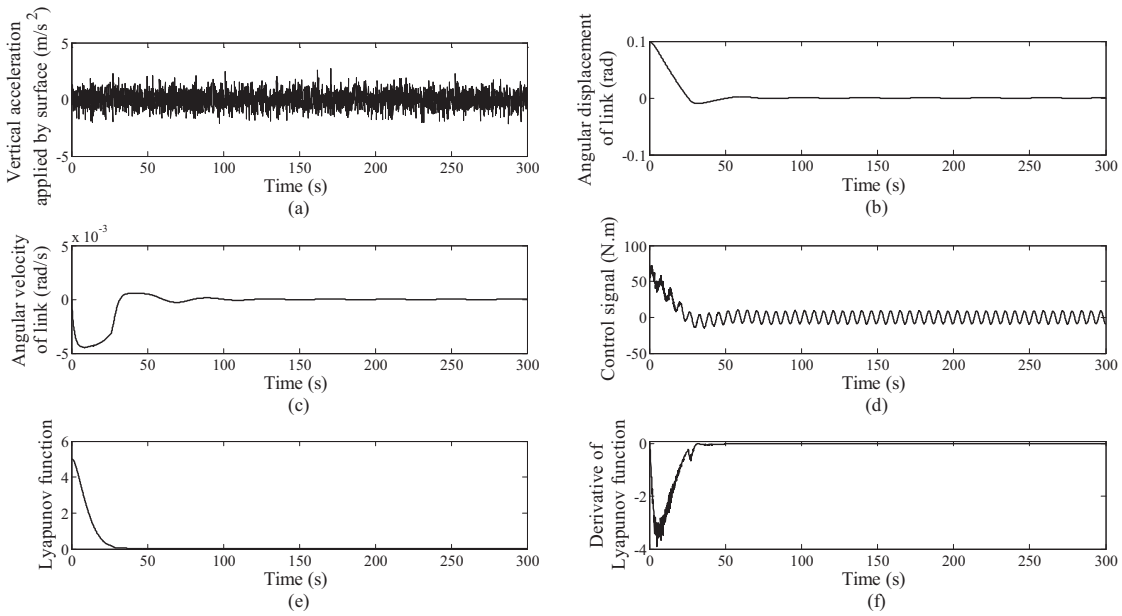


Fig. 6. Simulation results when Segway moves on a surface with random irregularities; scenario IV.

the control signal, proposed in (10), is a stabilizing feedback which guarantees the stability of the system.

5.5. Further discussions

In order to show how robust the proposed controller operates, three other simulations are performed while the vehicle moves on a surface given in Scenario IV. First, two different masses are considered as the combination of link and human. Results of both studies are illustrated in Fig. 7. As observed, the more value of the mass is, the larger the control torque will be required to keep the link and the rider close to the equilibrium point, in first 20 s of the simulation. Moreover, the Lyapunov and its time-derivative functions as well as the angular displacement of the link show that the system is robust against the variation of the mass m_l by applying the control law proposed in Eq. (10).

https://doi.org/10.1017/S0263574714000307 Published online by Cambridge University Press

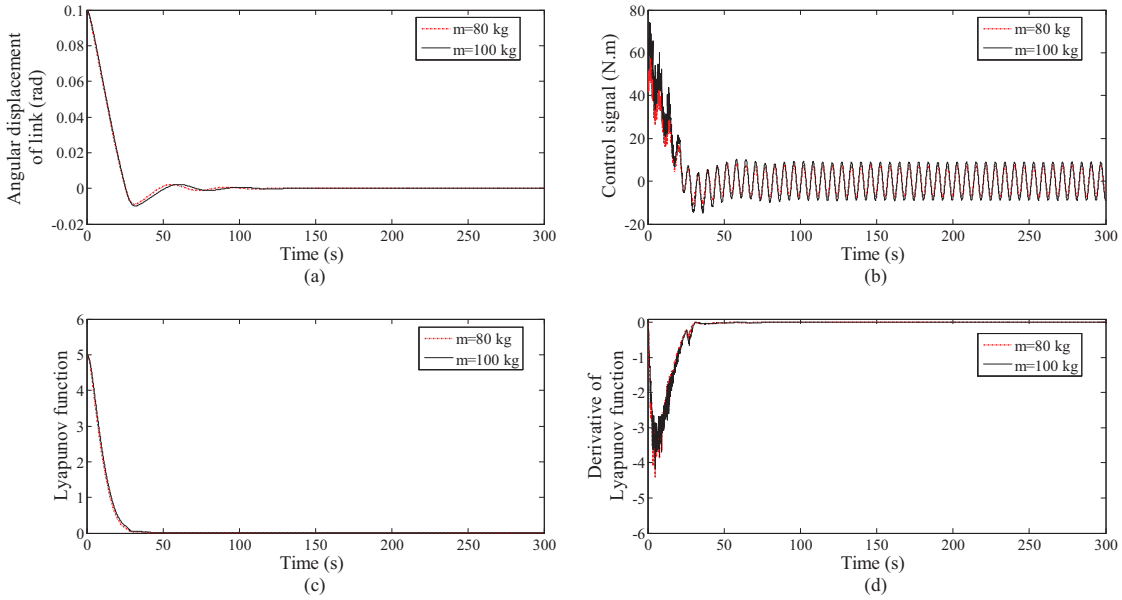


Fig. 7. (Colour online) Effect of mass of link and human on system response. Test is performed under characteristics presented for scenario IV.

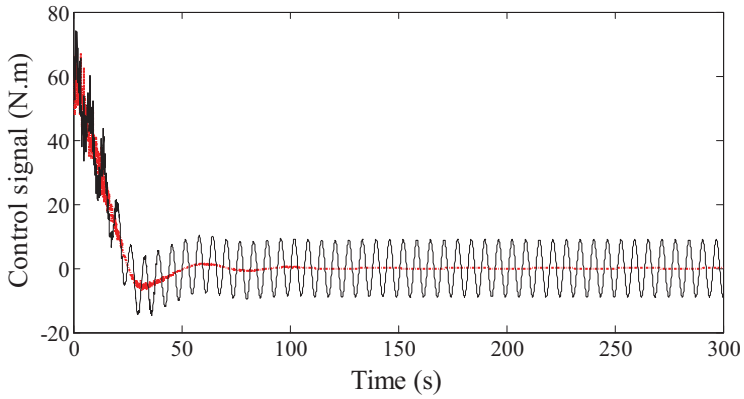


Fig. 8. (Colour online) Effect of angular acceleration of wheels on control signal. Dashed line (in red) indicates $\ddot{\varphi}_L = \ddot{\varphi}_R = 0$ and solid line (black) shows response when $\ddot{\varphi}_L = \ddot{\varphi}_R = \sin(t)$. Test is conducted under characteristics of scenario IV.

The effect of the angular acceleration of left and right wheels, $\ddot{\varphi}_L$,$\ddot{\varphi}_R$, on the performance of the control law is further investigated. The simulation study is carried out when $\ddot{\varphi}_L = \ddot{\varphi}_R = 0$ and $\ddot{\varphi}_L = \ddot{\varphi}_R = \sin(t)$. Results show that changing the angular acceleration of left and right wheels does not significantly affect the variation of angular displacement and velocity of the link as well as Lyapunov and its time-derivative functions. In order to avoid repetition, only the behavior of the control torque is shown in Fig. 8. With reference to this figure, it is found that the control signal is strictly affected by angular accelerations of wheels. The concept is also observed in Fig. 9 while the angular accelerations of wheels are set to random values.

As illustrated in Fig. 9, the control signal is robust against different random values for angular accelerations of wheels in which the control law (10) causes the position of the link to approach zero. The Lyapunov function and its derivative also stay positive and negative, respectively.

https://doi.org/10.1017/S0263574714000307 Published online by Cambridge University Press

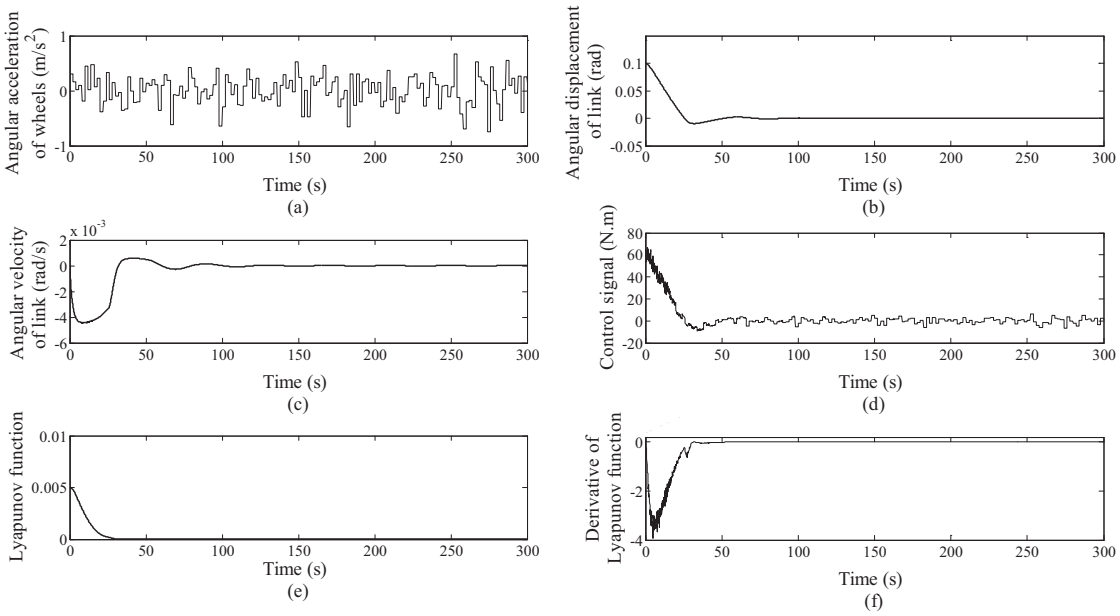


Fig. 9. Response of control signal under random values for wheels angular accelerations. Test is conducted under characteristics of scenario IV.

6. Conclusion

The purpose of this paper was to design and evaluate a control system for a two-wheeled self-balancing vehicle using the Lyapunov's feedback control design technique. Firstly, the control law of such a vehicle was derived in order to ensure the stability of the system. The existence of a sign function in the control law caused the control signal to behave discontinuously and nonsmoothly. Therefore, the existence, continuity, and uniqueness of Filippov's solution to the system were proven to keep further investigations on stability of the system. The asymptotic stability of the designed control system was also studied using the extensions of Lyapunov's stability theory to nonsmooth systems as well as the LaSalle's invariant set theorem. The effectiveness of the proposed controller was validated using simulation studies. The two-wheeled self-balanced vehicle was shown asymptotically stable, that is, the states converged to their equilibrium values. The proposed control law was found robust under different surface conditions, rider's mass as well as random angular acceleration of wheels. Future work should focus on stability analysis of the proposed controller on a real experimental setup.

References

1. Y. Maddahi, N. Sepehri, A. Maddahi and M. Abdolmohammadi, "Calibration of wheeled mobile robots with differential drive mechanisms: An experimental approach," *J. Robotica* **30**(6), 1029–1039 (2012).
2. Y. Maddahi, A. Maddahi and S. M. Hosseini Monsef, "Design improvement of wheeled mobile robots: Theory and experiment," *J. World Appl. Sci.* **16**(2), 263–274 (2012).
3. Segway Inc. Segway homepage. http://www.segway.com.
4. A. A. Saifizul, Z. Zainon, N. A. Abu Osman, C. A. Azlan and U. F. S. Ungku Ibrahim, "Intelligent control for self-erecting inverted pendulum via adaptive neuro-fuzzy inference system," *Am. J. Appl. Sci.* **3**(4), 1795–1802 (2006).
5. A. Mills, A. Wills and B. Ninness, "Nonlinear Model Predictive Control of an Inverted Pendulum," *American Control Conference* (2009) pp. 2335–2340.
6. K. Pathak, J. Franch and S. K. Agrawal, "Velocity Control of a Wheeled Inverted Pendulum by Partial Feedback Linearization," *IEEE Conference on Design and Control*, Atlantis (2004) pp. 3962–3967.
7. S. Iida and S. Yuta, "Control of a Vehicle Subsystem for an Autonomous Mobile Robot with Power Wheeled Steering", *Proceedings of IEEE International Workshop on Intelligent Motion Control* (1990) pp. 859–866.
8. Y. Ha and S. Yuta, "Trajectory tracking control for navigation of an inverted pendulum type self-contained mobile robot," *J. Robot. Auton. Syst.* **17**, 65–80 (1996).
9. F. Grasser, A. D'Arrigo, S. Colmbi and A. C. Rufer, "JOE: A mobile inverted pendulum," *IEEE Trans. Ind. Electron.* **49**(1), 107–114 (2002).

https://doi.org/10.1017/S0263574714000307 Published online by Cambridge University Press

10. H. J. Lee and S. Jung, "Gyro Sensor Drift Compensation by Kalman Filter to Control a Mobile Inverted Pendulum Robot System," *IEEE International Conference on Industrial Technology*, Gippsland (2009) pp. 1–6.
11. H. Azizan, M. Jafarinasab, S. Behbahani and M. Danesh, "Fuzzy Control Based on LMI Approach and Fuzzy Interpretation of the Rider Input for Two Wheeled Balancing Human Transporter," *IEEE Conference on Control and Automation*, Xiamen, China (2010) pp. 192–197.
12. C. Tsai, H. C. Huang and S. C. Lin, "Adaptive neural network control of a self-balancing two-wheeled scooter," *IEEE Trans. Ind. Electron.* **57**, 1420–1428 (2010).
13. L. Vermeiren, A. Dequidt, T. M. Guerra, H. R. Tirmant and M. Parent, "Modeling, control and experimental verification on a two-wheeled vehicle with free inclination: An urban transportation system," *J. Control Eng. Pract.* **19**, 744–756 (2011).
14. J. Aracil, J. Acosta and F. Gordillo, "A Controller for Swinging-up and Stabilization the Inverted Pendulum," *Proceeding of the 17th World Congress*, IFAC, Korea (2008).
15. A. Maddahi and A. H. Shamekhi, "Controller design for two-wheeled self-balancing vehicles using feedback linearisation technique," *Int. J. Veh. Syst. Modelling Test.* **8**(1), 38–54 (2013).
16. K. Zarei-nia, N. Sepehri and C. Q. Wu, "A Lyapunov controller for stable haptic manipulation of hydraulic actuators," *Int. J. Robust Nonlinear Control* **22**, 241–261 (2012).
17. A. F. Filippov, "Differential equations with discontinuous right-hand side," *Am. Math. Soc. Transl*. **42**, 199–231 (1964).
18. A. F. Filippov, "Differential equations with second members discontinuous on intersecting surfaces," *Differ. Equ.* **15**, 1292–1299 (1980).
19. Q. Wu and N. Sepehri, "On Lyapunov's stability analysis of non-smooth systems with applications to control engineering," *Int. J. Non-Linear Mech.* **36**(7), 1153–1161 (2001).
20. D. Shevitz and B. Paden, "Lyapunov stability theory of non-smooth systems," *IEEE Trans. Autom. Control* **39**(9), 1910–1914 (1994).
21. Q. Wu, N. Sepehri and A. B. Thornton-Trump, "An extended integral method to derive Lyapunov functions for nonlinear systems," *Int. J. Control* **62**(3), 717–736 (1995).
22. J. J. Slotine and W. Li, *Applied Nonlinear Control* (Prentice-Hall Inc., Englewood Cliffs, NJ, 1991).
23. J. LaSalle, "Some extensions of Liapunov's second method," *IRE Trans. Circuit Theory* **7**(4), 520–527 (1960).

Appendix - Fillipov's Conditions and Lemmas[17,18]

Condition A: The function $f(t,x_1,\ldots,x_n), i=1,2,\ldots,n \geq 1$ is a real-valued measurable function, defined almost everywhere in an open or closed domain Q of the space $(t,x_1,\ldots,x_n)$; for an arbitrary closed bounded region $D \subseteq Q$ there exist a function $A(t)$, finite almost everywhere, such that almost everywhere in D

$$|f(t,x_1,\ldots,x_n)| \prec A(t) \tag{A1}$$

Condition B: It is said that the system $f(t,x_1,\ldots,x_n)$ satisfies this condition in an open or closed region Q of the space t,x if the function $f(t,x)$ is defined almost everywhere in Q, is measurable, and for any bounded closed domain $D \subseteq Q$ there exist a summable function $B(t)$ such that almost everywhere in D, we have

$$|f(t,x_1,\ldots,x_n)| \prec B(t) \tag{A2}$$

Condition C: Consider the region G is formed of a finite number of regions $G_i (i = 1,2,\ldots,r)$ and the set of M shows the points of the boundaries of G_i. According to this condition, for all values of t except those in a finite set T of measure zero, each point (t,x) of the boundary of each G_i is also on the boundary of the section of this region by the plane $t =$ constant.

Theorem 4: Let the right hand side of function

$$\frac{\mathrm{d}x(t)}{\mathrm{d}t} = f(t,x_1,\ldots,x_n) \tag{A3}$$

be measurable in a region G, and satisfy inequality (A2) almost everywhere, where the function $B(t)$ is summable. Then for arbitrary initial conditions $x(t_0) = a$, where $(t_0,a) \in G$, a solution of Eq. (A3) exists satisfying these initial conditions and defined on the interval $[t_0 - d, t_0 + d]$, where d is such

https://doi.org/10.1017/S0263574714000307 Published online by Cambridge University Press

that the $(n + 1)$-dimensional "cylinder"

$$|t - t_0| \leq d, |x - a| \leq \left| \int_0^{t_0 \pm d} B(t)dt \right| \tag{A4}$$

is situated entirely inside G.

Theorem 5: Suppose that Eq. (A3) satisfies Condition B in the region Q. Then any solution $x(t)$ of it is continuable on the interval $[t_1,t_2]$ where either $t_2 = +\infty$ or for $t \to t_2 - 0$, we have one of three alternatives: *a*) $|x(t)| \to \infty$, *b*) $\rho \to 0$, where ρ is the distance from the point $(t,x(t))$ to the boundary of Q, *c*) $\lim |x(t)| \prec \infty$, $\lim \rho > 0$, $\lim (|x(t)| + {}^{1}\!/_{\rho}) = \infty$.

Lemma 9: Consider f^- and f^+ denote the limiting values of the vectors f when the system, shown in Eq. (A3), approaches to discontinuous surface, S, from G^- and G^+. If for $t_1 \prec t \prec t_2$, we have $f_N^+(t,x) > 0$, $f_N^-(t,x) > 0$ at all points of the piece S_0 of the surface S (or for these t we have $f_N^+(t,x) \prec 0$, $f_N^-(t,x) \prec 0$ at all points), then in the domain $G^- + S_0 + G^+$ we have uniqueness and continuous dependence of the solution on the initial conditions. $f_N(t,x)$ denotes the projection of the corresponding vector on the normal to surface S at the point $(t,x(t))$; the positive direction of the normal is always from G^- to G^+. The solution in this case, on the part S_0 of S, goes from G^- to G^+ and has only one point in common with S (respectively, goes from G^+ to G^-).

https://doi.org/10.1017/S0263574714000307 Published online by Cambridge University Press